PHYSICAL REVIEW E VOLUME 50, NUMBER 6 DECEMBER 1994

Subcritical-supercritical bifurcation crossover in directional solidification

D. Liu, L.M. Williams,* and H.Z. Cummins
Department of Physics, City College of the City University of New York, New York, New York 10031
(Received 18 March 1994)

The Mullins-Sekerka planar-cellular instability in directional solidification should be subcritical when the partition coefficient $k<0.45$ and latent heat is ignored. However, Merchant and Davis [Phys. Rev. Lett. **63**, 573 (1989)] predicted that as the solute concentration is reduced, the increasingly important thermal diffusion field would lead to a crossover from a subcritical to a supercritical bifurcation. We have performed directional solidification experiments on a series of succinonitrile samples containing different concentrations of Coumarin 152, and have found preliminary evidence for the predicted crossover at a concentration $C_t \sim 0.1\%$.

PACS number(s): 47.20.Hw, 47.20.Ky, 61.50.Cj

Equilibrium phase transitions with primary and secondary order parameters may exhibit a line of first-order transitions which passes through a tricritical point and becomes a line of second-order transitions. A similar phenomenon is possible in nonequilibrium dynamical systems. In this Rapid Communication we present preliminary evidence for a dynamical analogue of a tricritical point in the directional solidification instability.

Directional solidification of a dilute binary alloy at low growth speeds occurs with a stable, flat crystal-melt interface. At higher growth speeds a morphological instability occurs, and the initially flat interface transforms into a cellular (or dendritic) pattern [1,2]. A linear stability analysis for the two-dimensional case was first carried out in 1964 by Mullins and Sekerka [3], who examined the stability of the planar interface with respect to an infinitesimal perturbation of wave number q. Their analysis identified the wave number q_C of the initial instability and the critical pulling (growth) speed V_C above which the planar interface is unstable:

$$V_C=\frac{2DGk\kappa_L}{|m|C_\infty(1-k)(1+n)\kappa_L-kDL}\,, \tag{1}$$

where G is the temperature gradient, D the solute diffusion constant in the liquid, k the partition coefficient, m the liquidus slope, C_∞ the solute concentration in the liquid far ahead of the interface, L the latent heat, κ_L the thermal conductivity of the liquid, and n the solid-liquid thermal conductivity ratio. Equation (1) is a modified form of the constitutional supercooling criterion of Tiller *et al.* [4] which defines the onset of thermodynamic (as opposed to dynamical) instability. For growth speeds $V>V_C$, there is a band of unstable wave numbers whose width initially increases with increasing V, eventually decreasing again as the interface approaches restabilization. (The possible existence of a wavelength selection mechanism within this band is an unresolved problem [5].) The subcritical or supercritical nature of the Mullins-Sekerka planar-cellular bifurcation cannot be identified from the linear analysis.

Wollkind and Segel [6] carried out a (weakly) nonlinear extension of the Mullins-Sekerka analysis neglecting latent heat for one-dimensional deformations using a perturbation expansion, which gave a Landau equation of motion (i.e., an amplitude equation) for the amplitude ξ_q of a mode with wave number q:

$$d\xi_q/dt=a_0\xi_q-a_1\xi_q^3-a_2\xi_q^5+(\text{higher order terms}). \tag{2}$$

The linear growth rate coefficient a_0 is proportional to V, passing through $a_0=0$ at $V=V_C$ defined by Eq. (1). Equation (2) predicts different types of bifurcations, depending on the sign of a_1:

(i) $a_1>0$. The planar front is stable when $a_0<0$ and unstable when $a_0>0$. When $a_0>0$, ξ_q begins to grow from zero continuously and saturates to a stable solution of finite amplitude: $\xi_q=(a_0/a_1)^{1/2}$. The continuous bifurcation which occurs as a_0 changes from $a_0<0$ to $a_0>0$ is supercritical.

(ii) $a_1<0$. A finite jump from a planar interface to a cellular one may occur as a_0 approaches zero at a critical velocity below the threshold V_C given by the linear analysis. Since $a_1<0$, the next nonlinear term $a_2\xi_q^5$ is needed to obtain a finite-amplitude steady-state solution. This bifurcation is subcritical, and is expected to show both a discontinuous jump in amplitude and hysteresis within a range of speeds bounded by V_C^+ from above and V_C^- from below. Bifurcation diagrams for the two cases are shown in Fig. 1.

The calculation of a_1 was first performed by Wollkind and Segel [6] for the one-sided model, by Langer and Turski [7] and Ungar and Brown [8] for the symmetric model, and was extended by Caroli *et al.* [9] to the two-sided model. Caroli *et al.* found that for V and G both small, in the high-concentration case where the thermal conductivities are equal and latent heat can be neglected,

$$a_1\propto\frac{k^2+4k-2}{4k}\,, \tag{3}$$

*Present address: Center for Study of Gene Structure and Function, Hunter College—City University of New York, New York, NY 10021.

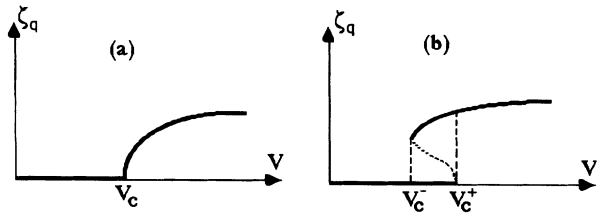

FIG. 1. Schematic bifurcation diagrams for the cellular interface amplitude ξ_q vs pulling speed V. (a) Supercritical bifurcation for $a_1>0$. (b) Subcritical bifurcation for $a_1<0$. The branches of stable solutions are indicated by heavy solid lines.

where the proportionality constant is always positive. Hence, with latent heat neglected, the nature of the transition only depends on the particular material via the value of the partition coefficient k. For $k>0.45$, $a_1>0$ and the bifurcation is supercritical; for $k<0.45$, $a_1<0$ and the bifurcation is subcritical.

Several experiments were carried out to test this prediction. Eshelman and Trivedi [10] performed experiments with succinonitrile (SCN)-acetone, and de Cheveigne *et al.* [11,12] performed experiments on CBr_4-Br_2. For these materials $k<0.45$, and both experiments indicated a subcritical bifurcation as predicted by Caroli *et al.* Bechhoefer and coworkers [13] studied a liquid crystal system with $k\sim 0.9$ and found that the bifurcation is supercritical, again as predicted. A summary of theoretical values of a_1 for a variety of materials was given by de Cheveigne *et al.* [14]. These measurements are very difficult, requiring long times to reach the steady state. The observations can also be complicated by three-dimensional effects, particularly in thick samples, as discussed by Cladis, Finn, and Gleeson [15].

Alexander *et al.* [16] included the latent heat in the condition describing the local balance of energy across the moving interface. Allowing for a finite latent heat results in a positive addition to the Landau coefficient a_1, and may therefore produce a supercritical bifurcation even though $k<0.45$, especially at low solute concentrations. Merchant and Davis [17,18] pointed out that by including latent heat in the analysis, the critical velocity for SCN-acetone is shifted significantly compared to that for $L=0$, bringing regions of supercritical bifurcation into an experimentally accessible parameter range. In the vicinity of $V=V_C$, a modified form of a_1 can be given in the low-pulling-speed limit [17]:

$$a_1\sim \frac{1-n+I^{-1}(n+1)}{(n+1)(1+I^{-1})\Gamma}, \tag{4}$$

where

$$I^{-1}=\frac{kDL}{(k-1)(1+n)\kappa_L m C_\infty} \tag{5}$$

is a latent-heat parameter, and

$$\Gamma=\frac{\gamma T_m k V}{Lm(k-1)C_\infty D} \tag{6}$$

is a scaled surface energy. T_m is the melting point of the pure solvent, and γ is the surface tension.

As noted by Merchant and Davis [17], if $1-n$ is far from zero, latent-heat effects are not very important. However, if $n\approx 1$, as in plastic crystals, the magnitude, and indeed the sign of a_1 is very sensitive to latent-heat effects. As a result, the impurity concentration of the solute C_∞ becomes crucial in determining the sign of a_1. With decreasing C_∞, the thermal field becomes increasingly important; a_1 should change sign from negative to positive at a crossover concentration C_t, where the subcritical bifurcation for $C>C_t$ will change into a supercritical bifurcation for $C<C_t$.

The maximum possible hysteresis $\Delta V_{\max}=V_C^+-V_C^-$, set by the limits of stability of the planar and cellular interfaces, is given by

$$\Delta V_{\max}=\begin{cases} a_1^2/4a_2 s, & a_1<0 \\ 0, & a_1>0 \end{cases} \tag{7}$$

where s is the slope of $a_0(V)$ at $V=V_C$.

To study the instability of a planar crystal-melt interface and the planar-cellular bifurcation, two key experimental factors must be satisfied: (i) a precise linear motion and a stable temperature gradient are required, (ii) a pure plastic crystal (in our case succinonitrile) mixed with an accurately known amount of impurity [in our case Coumarin152 (C152)] at low concentrations (less than 0.5 wt %) must be prepared. Since the critical velocity for the bifurcation in this system is of order 1 μm/s, and the crossover of the subcritical to supercritical bifurcation occurs as the concentration decreases, very small deviations from pulling speed linearity or stability, or uncontrolled impurity concentrations, can cause significant variations and mask the phenomena under study.

We have designed and constructed a precision directional solidification apparatus based on the directional solidification stage of Jackson and co-workers [19]. The apparatus consists of a motorized translation stage to pull the sample capillary and a crystal growth chamber to provide the temperature gradient, all contained in a Lucite case that provides thermal isolation. The apparatus is mounted on the stage of a Nikon Diaphot microscope equipped with a Dage-MTI charge-coupled-device videocamera for digital image acquisition.

The central part of the crystal growth chamber is a rectangular stainless steel tunnel with sapphire windows. This tunnel is sandwiched between copper cold and hot blocks whose temperatures are controlled to better than $\pm$ 0.01 K. Two guides are precisely located to ensure accurately coaxial motion of the sample. Mineral oil is used to fill the tunnel for uniform thermal conduction and for optical matching. The top section of the hot block is elongated to keep the entire liquid side of the interface molten, maintaining an initial uniform dye concentration on the whole liquid side of the interface. The gap between the cold and hot blocks can be adjusted from 0.48 to 0.95 cm for temperature gradients up to several hundred degrees per centimeter (typically 100 K/cm). In this experiment the gap was 0.48 cm.

The motion control system is a MicroMo dc servo motor with a Hewlett-Packard integral optical encoder controlled by a MicroMo Unicontroller series MCX-02. The controller is connected to a Macintosh II computer which provides programmable precision position and velocity control. A precision Velmex Unislide translation stage is used to convert the motion from rotational to translational. The translational ve-

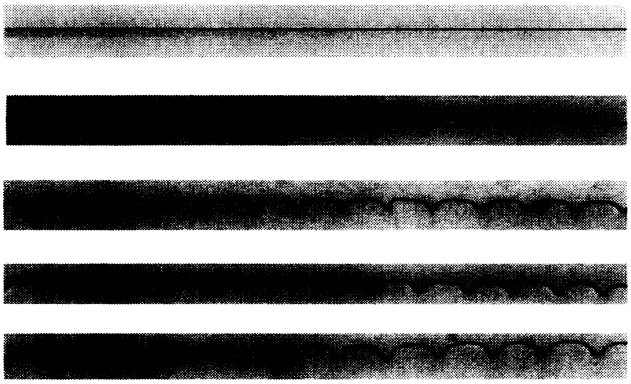

FIG. 2. Interface profiles after restabilization following the initial instability. The top reference image is of a planar interface at rest. The four following images are for C = 0.019, 0.062, 0.130, and 0.236 wt %, with $G = 100$ K/cm.

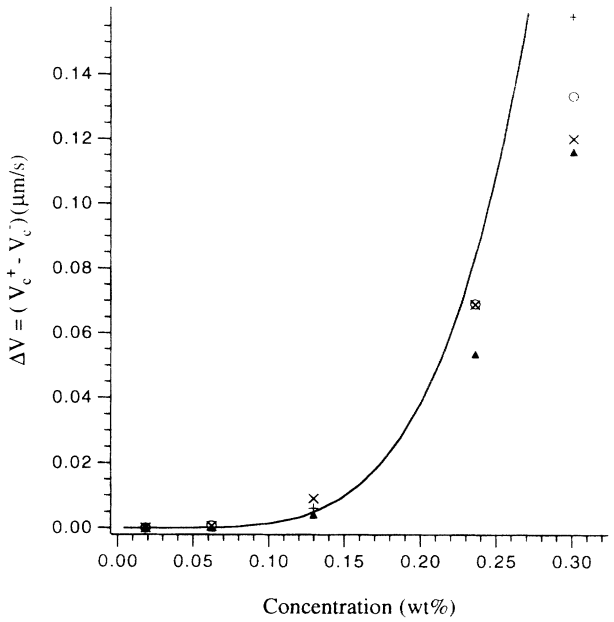

FIG. 3. Observed hysteresis ΔV for SCN-C152 samples with G = 52 K/cm. The five groups of points correspond to C = 0.019, 0.062, 0.130, 0.236, and 0.301 wt %. For these samples, average values of V_C^+ were 9.5, 1.7, 0.95, 0.64, and 0.85 μm/s, respectively. Different symbols represent individual experimental runs. The solid curve was calculated from Eq. (7) using measured thermodynamic parameters for SCN-C152 to compute a_0 and a_1, with a_2 arbitrarily fixed at 400.

locity of the capillary was found to be constant to within 1%. The velocity increment can be programmed to be as small as needed (typically 0.03 μm/s). The free travel distance of the capillary is 72 mm.

A series of succinonitrile-Coumarin152 samples was prepared with C152 concentration between 0.01 and 0.43 wt %. The succinonitrile (purchased from Fluka) was vacuum distilled four times before adding carefully weighed C152 (purchased from Sigma). The sample holders—2 mm$\times$100 μm (inside dimension) glass capillaries purchased from Vitro Dynamics—were cleaned with hot detergent solution, acetone, and chromic acid and rinsed with distilled water, baked dry under vacuum overnight, and finally flame sealed at both ends for storage. The well-mixed SCN-C152 mixture was then loaded under vacuum into these cleaned glass capillaries, avoiding exposure to air and water vapor, which were then again flame sealed. The sample ($\sim$16 cm long) was kept under vacuum during the whole preparation process, except for a brief pressurization with He gas to force the solution into the capillary. The final concentration of C152 was then calibrated by fluorescence measurements.

An argon laser with a fiber-optic coupling and focusing mechanism was employed to obtain a well-oriented single crystal sample, exploiting the optical absorption of the laser dye Coumarin152 used as the second component. After the initial solidification, we used the laser to melt all the grains except one, which was then reduced to a sufficiently small size. This procedure was repeated until a single well-oriented crystal was obtained.

Our experiments were carried out in a temperature gradient of either 52 or 100 K/cm. Before each experiment, the sample was equilibrated in the temperature gradient at least overnight. The pulling speed V was increased gradually in small increments until the planar interface became unstable at $V \sim V_C^+$. (For these samples V_C^+ ranged from 0.5 to 13.15 μm/s.) Typical waiting times between V steps were $\sim$2 h. As previously found by other authors, the instability originated in one or more localized regions and spread laterally across the interface. The spreading occurs more rapidly for the higher concentration samples. Figure 2 illustrates the restabilized interface following the planar-cellular bifurcation for four samples with different C152 concentrations. The measured wavelengths ranged from 89 μm ($C = 0.019$) to 107 μm ($C = 0.236$). The Mullins-Sekerka prediction is $\sim$1.5 times larger, as found in previous experiments [10,11,14]. After recording the interface profile, the pulling speed was then increased well above V_C^+ to make sure the system enters the cellular regime completely and was then slowly decreased in small increments until a cellular-planar bifurcation occurred at $V \sim V_C^-$. Several such runs were performed for each sample in order to determine the hysteresis $\Delta V = V_C^+ - V_C^-$. The resulting ΔV values are shown in Fig. 3. For the $C = 0.019$ and 0.062 wt % samples, $\Delta V = 0$ within experimental error. For the samples with low SCN concentrations ($\lesssim$0.02 wt %) where V_C^+ was large, grain boundaries tended to appear as the growth speed approached V_C^+.

We have performed a preliminary calculation of a_0 and a_1 for SCN-C152 and plotted Eq. (7) and our experimental data in Fig. 3. In the calculation we used standard thermodynamic parameters for SCN [14] with values we determined [20] for $m = -1.65$ K/wt %, $D = 2.5 \times 10^{-6}$ cm^2/s, and $k = 0.05$. We also used the approximate expression of Eq. (4) for a_1, rather than the full expression of Ref. [16]. Since the value of the dimensionless a_2 was not known, we assumed it to be constant and fixed it arbitrarily at a_2 = 400. (Detailed calculations will be presented in a future article.) As we can see in Fig. 3, at high concentrations there is always some velocity hysteresis, characteristic of a subcritical bifurcation. But as the concentration decreases, this hysteresis decreases monotonically and eventually vanishes, as predicted by Merchant and Davis. The subcritical-

supercritical crossover where $a_1 = 0$ takes place at a concentration $C_t \sim 0.1$ wt %. The scatter observed in different runs for a particular sample is expected, since ΔV_{max} of Eq. (7) is an upper limit to ΔV_{expt}. Also, as seen in Fig. 2, at low concentrations the cellular interface restabilizes at very small amplitudes as expected for a supercritical bifurcation, while at high concentrations a large amplitude cellular pattern appears, characteristic of a subcritical bifurcation.

The results illustrated in Figs. 2 and 3 suggest that a subcritical-supercritical crossover occurs in SCN-C152 with decreasing C152 concentration, as predicted by Merchant and Davis [17]. In this preliminary experiment, however, we have not been able to verify agreement between predicted and observed values of V_C^+, nor to rule out the possibility that transverse deformations of the front play a role in the instability [21].

Note added. We have recently realized that a subcritical-supercritical bifurcation crossover in the Couette-Taylor hydrodynamic instability was reported by A. Aitta, G. Ahlers, and D. S. Cannell [Phys. Rev. Lett. **54**, 673 (1985)].

We acknowledge helpful discussions and correspondence with C. Caroli, S.H. Davis, W.J. Rappel, G. Faivre, S. Akamatsu, and M. Ben Amar. This research was supported by the U.S. Dept. of Energy under Grant No. DE-FG02-84ER45132.

[1] J.S. Langer, Rev. Mod. Phys. **52**, 1 (1980).
[2] S.R. Coriell, G.B. McFadden, and R.F. Sekerka, Ann. Rev. Mater. Sci. **15**, 119 (1985).
[3] W.W. Mullins and R.F. Sekerka, J. Appl. Phys. **35**, 444 (1964).
[4] W.A. Tiller, K.A. Jackson, J.W. Rutter, and B. Chalmers, Acta Metall. **1**, 428 (1953).
[5] M. Ben Amar and B. Moussallam, Phys. Rev. Lett. **60**, 317 (1988)
[6] D.J. Wollkind and L.A. Segel, Philos. Trans. R. Soc. A **268**, 351 (1970).
[7] J.S. Langer and L.A. Turski, Acta Metall. **25**, 1113 (1977).
[8] L.H. Ungar and R.A. Brown, Phys. Rev. B **29**, 1367 (1984).
[9] B. Caroli, C. Caroli, and B. Roulet, J. Phys. (Paris) **43**, 1767 (1982). (This paper contained a minor error, subsequently corrected by Wollkind *et al.* [22], which does not change the qualitative conclusions.)
[10] M.A. Eshelman and R. Trivedi, Acta Metall. **35**, 2443 (1987).
[11] S. de Cheveigne, C. Guthmann, and M.M. Lebrun, J. Cryst. Growth **73**, 242 (1985).
[12] S. de Cheveigne, C. Guthmann, and M.M. Lebrun, J. Phys. (Paris) **47**, 2095 (1986).
[13] J. Bechhoefer, P. Oswald, A. Libchaber, and C. Germain, Phys. Rev. A **37**, 1691 (1988).
[14] S. de Cheveigne, C. Guthmann, P. Kurowski, E. Vicente, and H. Biloni, J. Cryst. Growth **92**, 616 (1988).
[15] P.E. Cladis, P.L. Finn, and J.T. Gleeson, in *Nonlinear Evolution of Spatio-Temporal Structures in Dissipative Continuous Systems*, edited by F.H. Busse and L. Kramer (Plenum Press, New York, 1990), p. 457.
[16] J.I.D. Alexander, D.J. Wollkind, and R.F. Sekerka, J. Cryst. Growth **79**, 849 (1986).
[17] G.J. Merchant and S.H. Davis, Phys. Rev. Lett. **63**, 573 (1989).
[18] G.J. Merchant and S.H. Davis, Phys. Rev. B. **40**, 11 140 (1989).
[19] K.A. Jackson and J.D. Hunt, Acta Metall. **13**, 1212 (1965); Trans. Met. Soc. AIME **236**, 1129 (1966); J.D. Hunt, K.A. Jackson, and H. Brown, Rev. Sci. Instrum. **37**, 805 (1966).
[20] L.M. Williams, M. Muschol, X. Qian, W. Losert, and H.Z. Cummins, Phys. Rev. E **48**, 489 (1993).
[21] Such transverse deformations have been shown to occur in CBr_4 samples with thicknesses above 50 μm [G. Faivre, S. Akamatsu, and C. Caroli (private communication)].
[22] D.J. Wollkind, D.B. Oulton, and R. Sriranganathan, J. Phys. (Paris) **45**, 505 (1984).

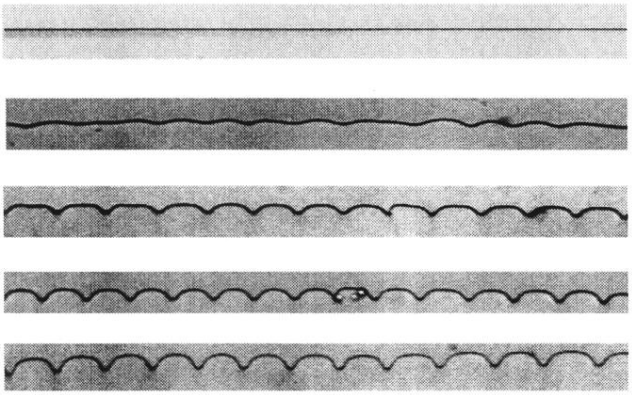

FIG. 2. Interface profiles after restabilization following the initial instability. The top reference image is of a planar interface at rest. The four following images are for $C = 0.019$, 0.062, 0.130, and 0.236 wt %, with $G = 100$ K/cm.